OFFICE OF NAVAL RESEARCH

Contract N00014-88-AF-00001

R&T Code 413d001---03

TECHNICAL REPORT NO. 33

Low Frequency Dielectric Properties of Polyether Electrolytes

by

John J. Fontanella & Mary C. Wintersgill

Prepared for Publication

in

Polymer Electrolyte Reviews - 2.

U. S. Naval Academy
Department of Physics
Annapolis, MD 21402-5026

June 1988

Unclassified
SECURITY CLASSIFICATION OF THIS PAGE

REPORT DOCUMENTATION PAGE

1a. REPORT SECURITY CLASSIFICATION: Unclassified	1b. RESTRICTIVE MARKINGS
2a. SECURITY CLASSIFICATION AUTHORITY	3. DISTRIBUTION/AVAILABILITY OF REPORT: This document has been approved for public release and sale; its distribution is unlimited.
2b. DECLASSIFICATION/DOWNGRADING SCHEDULE	
4. PERFORMING ORGANIZATION REPORT NUMBER(S): 33	5. MONITORING ORGANIZATION REPORT NUMBER(S)
6a. NAME OF PERFORMING ORGANIZATION: U. S. Naval Academy; 6b. OFFICE SYMBOL (If applicable)	7a. NAME OF MONITORING ORGANIZATION
6c. ADDRESS (City, State, and ZIP Code): Physics Department, Annapolis, MD 21402-5026	7b. ADDRESS (City, State, and ZIP Code)
8a. NAME OF FUNDING/SPONSORING ORGANIZATION: Office of Naval Research; 8b. OFFICE SYMBOL (If applicable): ONR	9. PROCUREMENT INSTRUMENT IDENTIFICATION NUMBER
8c. ADDRESS (City, State, and ZIP Code): 800 N. Quincy Street, Arlington, VA 22217-5000	10. SOURCE OF FUNDING NUMBERS

PROGRAM ELEMENT NO.	PROJECT NO.	TASK NO.	WORK UNIT ACCESSION NO
61153N	RR013-06-0C	627-793	

11. TITLE (Include Security Classification): Low Frequency Dielectric Properties of Polyether Electrolytes. (Unclassified)

12. PERSONAL AUTHOR(S): John J. Fontanella and Mary C. Wintersgill

13a. TYPE OF REPORT	13b. TIME COVERED	14. DATE OF REPORT (Year, Month, Day)	15. PAGE COUNT
Interim	FROM 87/10/1 TO 88/9/30	June 1988	30

16. SUPPLEMENTARY NOTATION

17 COSATI CODES			18. SUBJECT TERMS (Continue on reverse if necessary and identify by block number)
FIELD	GROUP	SUB-GROUP	Prepared for publication in Polymer Electrolyte Reviews - 2. (Unclassified)

19. ABSTRACT (Continue on reverse if necessary and identify by block number)

Beyond their interest as fundamental properties of a material, the dielectric constant and loss are of particular significance for ion conducting polymers. For example, the dielectric constant plays a fundamental role in the ability of a polymer to dissolve salts. The reason is that the dielectric constant is a measure of the reduction of Coulomb interactions and thus high dielectric constant fluids greatly reduce ion-ion interactions, inhibiting crystal formation. The dielectric loss

20. DISTRIBUTION/AVAILABILITY OF ABSTRACT	21. ABSTRACT SECURITY CLASSIFICATION
☒ UNCLASSIFIED/UNLIMITED ☐ SAME AS RPT ☐ DTIC USERS	Unclassified

22a. NAME OF RESPONSIBLE INDIVIDUAL	22b. TELEPHONE (Include Area Code)	22c. OFFICE SYMBOL
John J. Fontanella	301-267-3437	

is interesting as it probes a wide variety of phenomena including the electrical conductivity along with any relaxations which may be present in the material including that associated with the glass transition. Consequently, it is worth reviewing some of what is known concerning the dielectric properties of these materials. The discussion will be limited to poly(ethylene oxide) (PEO) and poly(propylene oxide) (PPO).

LOW FREQUENCY DIELECTRIC PROPERTIES OF POLYETHER ELECTROLYTES

Mary C. Wintersgill and John J. Fontanella

Physics Department

U.S. Naval Academy

Annapolis, MD, USA 21402-5026

1. INTRODUCTION

Beyond their interest as fundamental properties of a material, the dielectric constant and loss are of particular significance for ion conducting polymers. For example, the dielectric constant plays a fundamental role in the ability of a polymer to dissolve salts. The reason is that the dielectric constant is a measure of the reduction of Coulomb interactions and thus high dielectric constant fluids greatly reduce ion-ion interactions, inhibiting crystal formation.[1] The dielectric loss is interesting as it probes a wide variety of phenomena including the electrical conductivity along with any relaxations which may be present in the material including that associated with the glass transition. Consequently, it is worth reviewing some of what is known concerning the dielectric properties of these materials. The discussion will be limited to poly(ethylene oxide) (PEO) and poly(propylene oxide) (PPO).

2. DEFINITIONS AND BASIC CONCEPTS

The best approach to the dielectric constant is via the polarization vector (dipole moment per unit volume):[2]

$$\underset{\sim}{P} = \varepsilon_o \chi_e \underset{\sim}{E} \qquad (1)$$

where ε_o is the permittivity of free space, χ_e is the electric susceptibility, and $\underset{\sim}{E}$ is the electric field. Next, the electric displacement vector, $\underset{\sim}{D}$, is defined to be:

$$\underset{\sim}{D} = \varepsilon_o \underset{\sim}{E} + \underset{\sim}{P} \qquad (2)$$

from which it follows that:

$$\underset{\sim}{D} = \varepsilon_o(1 + \chi_e)\underset{\sim}{E} \qquad (3)$$

which leads to the definition of the real part of the dielectric constant (relative permittivity), ε', as:

$$\varepsilon' = 1 + \chi_e \qquad (4)$$

so that:

$$\underset{\sim}{D} = \varepsilon_o\varepsilon'\underset{\sim}{E} \qquad (5)$$

The imaginary part of the dielectric constant, ε'', is related to the electrical conductivity, σ, which is defined by:

$$\underset{\sim}{J} = \sigma\underset{\sim}{E} \qquad (6)$$

where $\underset{\sim}{J}$ is the electric current density. The definition of ε'' follows from Maxwell's equation (in this case written for harmonic fields):

$$\underset{\sim}{\nabla} \times \underset{\sim}{H} = j\omega\underset{\sim}{D} + \underset{\sim}{J} \qquad (7)$$

where $\underset{\sim}{H}$ is usually known as the magnetic field intensity. Substituting, then,

$$\underset{\sim}{\nabla} \times \underset{\sim}{H} = (j\omega\varepsilon_o\varepsilon' + \sigma)\underset{\sim}{E} \qquad (8)$$

and thus

$$\underset{\sim}{\nabla} \times \underset{\sim}{H} = j\omega\varepsilon_o(\varepsilon' - j\sigma/\varepsilon_o\omega)\underset{\sim}{E} \qquad (9)$$

from which the definition:

$$\varepsilon'' = \sigma/\varepsilon_o\omega \qquad (10)$$

follows in order to define the complex dielectric constant:

$$\varepsilon^* = \varepsilon' - j\varepsilon'' \qquad (11)$$

Often, the loss tangent:

$$\tan\delta = \varepsilon''/\varepsilon' = \sigma/\varepsilon_o\omega\varepsilon' \qquad (12)$$

is also defined which is a measure of the ratio of the conduction current relative to the displacement current. It is important to realize, then, that the true real part of the dielectric constant arises from the

polarization of the material as given by Eq. (1).

Often, confusion concerning the dielectric constant arises because of the operational definition of the real part of the dielectric constant (which is here designated as the apparent dielectric constant), which is:

$$\varepsilon'_{app} = C/C_o \qquad (13)$$

where C_o is the capacitance of any configuration of electrodes where the space surrounding them is vacuum and C is the capacitance with an isotropic material filling the space. The confusion arises because charges which are free to move within the material, but are blocked at the electrodes, can give a large contribution to the capacitance measured by an instrument. This has been referred to as space charge polarization and is often observed in ionic conductors.[3] (In the case of lanthanum fluoride, the polarization effects are apparently due to surface effects.[4]) As this contribution is a consequence of the ionic conductivity, it will be both frequency and temperature dependent. Specifically, the apparent dielectric constant will decrease as frequency increases and will decrease as temperature decreases. The reason for identifying this false contribution to the dielectric constant in the case of polymers, of course, is that it does not contribute to the solvation characteristics of the material.

The operational definition of the imaginary part of the dielectric constant is often taken to be:

$$\varepsilon'' = G/\omega C_o \qquad (14)$$

where G is the conductance of the material. Consequently, G/ω differs from ε'' only via ε_o and the geometrical factor contained in C_o. There

are no ambiguities associated with this definition of ε'' other than those associated with separating the various contributions which again can be done via the frequency and temperature dependence.

3. Poly(ethylene oxide) and Poly(propylene oxide)

A plot of the "apparent" real and imaginary parts of the dielectric constant for PEO vs. temperature is shown in Fig. 1. The two relaxation regions usually seen[5-18] in this material, α_a and γ, are apparent in the imaginary parts along with their contributions to the real part of the dielectric constant.

As regards its impact on the solubility of ions in PEO, the real part of the dielectric constant is an extremely important component of these results. The false part of the dielectric constant, that due to space charge or surface effects is apparent at high temperatures. As discussed in section 2, it is identifiable by its strong frequency and temperature dependence. It is seen to be insignificant below the glass transition temperature. Qualitatively subtracting off this contribution, the dielectric constant of the solid at about room temperature is approximately 4. Aside from a possible small contribution from the α_c relaxation, this represents the dielectric constant of typical PEO at room temperature. This implies very little reduction of ion-ion interactions and thus raises the question of why PEO has such an afinity for ions. The answer can be found in the data of Porter and Boyd[13] who studied the dielectric constant of both molten and solid PEO. Their data are shown in Fig. 2 and it is seen that the dielectric constant of molten, and hence amorphous PEO is approximately 8. This shows at least part of the reason why PEO is a fairly effective solvent for a large number of salts.

This line of reasoning can be pursued further by considering the dielectric constant of PPO which is shown in Fig. 3.[19,20] The data are

similar to that reported by Varadarajan and Boyer[21]. The differences may be due to the fact that those authors studied low molecular weight (3034) material while the present work is for PAREL 58 elastomer (Hercules, Inc.) which is a high molecular weight material which contains about 5% of allyl glycidyl ether. However, the differences are within the approximately 15% uncertainty of the absolute dielectric constant for the present work. The relative variation with temperature or frequency is accurate at about the 0.1% level. It is apparent that the dielectric constant of about 5.5 is smaller than for amorphous PEO. This is a consequence of the methyl group making PPO less polar than PEO and correlates with the fact that PPO is not as strong a solvent as PEO. In fact, it has been recently shown[20,22-24] that at elevated temperatures salts have a tendency to precipitate out of PPO. Indeed, it has been observed[20] that the higher the melting point of the salt, the lower the salt precipitation temperature implying that the stronger the ion-ion interaction, the easier it is for the salt to precipitate out. In ref. 20 it was pointed out that the variation of the dielectric constant with temperature shown in Fig. 3 can be used to explain the effect. Specifically, it is seen that the dielectric constant decreases as temperature increases in PPO and thus screening of the Coulomb interaction becomes weaker as temperature increases.

For PEO, the variation of the dielectric constant with temperature within the amorphous phase is not clear at the present time. Before the crystalline phase melts, the dielectric constant of the bulk material actually increases with increasing temperature. This is apparent from Fig. 1a and is expected in that the strength of the loss peak associated with the glass transition, α_a, increases as temperature increases as seen in

Fig. 1b. This behavior often occurs in semicrystalline polymers. However, the variation of the dielectric constant with temperature above the melting point remains to be determined. It is likely that it will behave similarly to the results for PPO shown in Fig. 3 where Curie-Weiss behavior is seen i.e. both the loss peak and dielectric constant decrease approximately as 1/T. In any event salt precipitation, if it occurs, will take place at higher temperatures than in PPO because of the higher dielectric constant of PEO.

It has been well established that the α_a relaxation in PEO and the α relaxation in PPO are associated with the glass transition.[1-3] For example, for typical loss peaks as shown in Fig. 4, it has been shown[25] that the peak position, which is approximately equal to the reciprocal of the relaxation time, follows a VTF equation:

$$\omega_p = AT^{-1/2} \exp^{-[E_a/k(T-T_o)]} \qquad (15)$$

T imaginary part of the Havriliak-Negami function[26] for the complex capacitance, $C^*=C-jG/\omega$:

$$C^* = \frac{D}{[1 + (i\omega\tau_o)^{(1-\alpha)}]^{\beta}} \qquad (16)$$

was best-fitted to the data in order to determine the peak positions. Typical results are shown in Fig. 4. For the three temperatures, the three constant Havriliak-Negami parameters were found to be D=6.4, α=.25, and β=0.53 while τ_o varied from 1.84×10^{-5}s to 4.79×10^{-4}s to 5.27×10^{-3}s for 230.8K, 221.8K, and 215.8K respectively. By fitting Eq. (15) to the

relaxation time data, it was found that E_a=0.059 eV, T_o=[illegible].5K.[15], and $\log_{10}A$=13.95$K^{1/2}\Omega^{-1}cm^{-1}$. These parameters are important for comparison with the results for the ionic conductivity as discussed in section 4.

Another indication that the α relaxation is associated with the glass transition temperature, is that these relaxations are strongly dependent upon pressure as is usually the case for glass transition temperatures. The data for PEO[27] and PPO[28] are shown in Figs. 5 and 6, respectively. From the data it was concluded that the alpha relaxations and hence the glass transition temperatures shift about 9 ^{o}C/kbar for PEO and 17 ^{o}C/kbar for PPO. These values are typical for glass transitions in polymers.

To analyze the data from an isothermal point of view is also useful. However, the loss peak vs. frequency is not observable for PEO at the frequencies used in the present work. This is expected on the basis of the data for PEO presented by Connor et al.[9] Consequently, such results can only be presented for PPO. In that case, the quantity usually used to describe these processes is the activation volume, which is defined by:

$$\Delta v = (\partial g/\partial P)_T \qquad (17)$$

where g is the Gibbs energy for the process in question. In order to treat the α_a relaxation properly, a free volume expression such as Eq. (15) should be used. The difficulty is to identify the Gibbs energy. One such model[29] contains the requisite form, however, there are a large number of ambiguities associated with the other terms such as the entropy and other constants. For example, Papke et al.[29] arrived at an expression for the free volume activation volume for electrical conductivity, but did not take into account that T_o is likely to be strongly pressure dependent. A more

correct expression exists[30] and, in fact, was used to show that T_o cannot be equal to the glass transition temperature. That result has since been verified by careful fitting of electrical conductivity data.[25,28] However, in view of the remaining ambiguities, that approach will not be considered further until a more complete free volume theory exists.

Alternatively, an "Arrhenius" activation volume can be calculated via:

$$\Delta v_{Arr} = -kT(\partial \ln \omega_p / \partial P)_T \qquad (18)$$

The reason that this is called an Arrhenius activation volume is that it is based on the assumption of Arrhenius behavior which, of course, is not really valid for these materials as Eq. (18) follows from (17) under the assumption that the process is described by:

$$\omega_p = c \; EXP(-g/kT) \qquad (19)$$

where c is a pressure independent constant.

The large Arrhenius activation volumes, 46-81 cm^3/mol, calculated from Eq. (18) are understandable in that the relaxation is controlled by the large scale segmental motions of the polymer chain involved in the glass transition[25] i.e. large numbers of atoms are involved in the reorientation process and thus a large volume change of the material is necessary as the dipoles proceed from the minimum energy position to the saddle point.

This is in contrast to results for the γ relaxation for PEO for which the activation volume is found to be very small[27,31], on the order of 4 cm^3/mol. This is consistent with the usual interpretation of γ as due to the motion of very small segments of the polymer chain[33-34]. It is interesting that these motions are associated with the amorphous phase and

persist above the glass transition and into the molten region for PEO.[13] It has been shown that the process exhibits Arrhenius behavior with an activation energy of about 0.33 eV. Further, Rietman et al.[35] have pointed out that a nuclear magnetic resonance signal with a similar activation energy exists in these materials[36]. This signal is probably correlated with the γ relaxation. It follows that the motions represented by this process must be included in any complete theory of ion conduction in these materials.

There is another relaxation which is often observed in PEO. That relaxation is either labeled α_c[17,37-39] or merely α[40] which occurs at a higher temperature (or lower frequency) than α_a. That relaxation is easily seen in the thermally stimulated depolarization current (TSDC) results shown in Fig. 7. TSDC is essentially a very low frequency (on the order of mHz) dielectric relaxation experiment. That relaxation is somehow related to the crystalline phase. However, Porter and Boyd[13] were not able to identify such a relaxation in PEO.

4. PEO and PPO Containing Ions

Of most interest when salts are added to the polyethers, of course, is the electrical conductivity. Insight into the conductivity can be obtained from a study of the α relaxation. Specifically, it is clear that for amorphous polymers the electrical conductivity exhibits VTF type behavior and thus an equation similar to Eq. (15) is appropriate, namely,

$$\sigma = AT^{-1/2} \exp^{-[E_a/k(T-T_o)]} \qquad (20)$$

By fitting Eq. (20) to the electrical conductivity data for PPO containing various lithium salts, it was found[25] that the activation parameters, E_a and T_o, are very close to for those obtained for the electrical relaxation time for the α relaxation. For example, for PPO-$LiCF_3SO_3$ E_a=0.086 eV and T_o=214K is 34°C lower than the central glass transition temperature.[25] To emphasize the correlation, this best fit curve for the electrical conductivity is plotted in Fig. 8 along with the conductivity and data for the α relaxation. It is seen that the peak positions can be scaled to follow the same VTF curve as the electrical conductivity. Consequently, this represents evidence that the dominant process controlling the ionic conductivity is the same as that for the α relaxation. Since it has been known for many years that the α relaxation is controlled by large scale segmental motions of the polymer chains, that must also be the dominant process controlling ionic conductivity in amorphous polymers. Of course, this alone does not imply that large scale segmental motions represent the transport mechanism, because the electrical conductivity does not

distinguish between ion concentration and mobility. However, using ^{23}Na NMR techniques on PPO containing $NaClO_4$ it has been shown that over a temperature range where the conductivity changes by five orders of magnitude the carrier concentration changes by only a small amount (about 20%).[23] Consequently, carrier generation plays only a minor role in the variation of electrical conductivity with temperature. The combined results show, then, that the dominant process controlling ion motion is indeed large scale segmental motion of the polymer chains.

A similar correlation exists for the effect of pressure on the electrical relaxation time for the α relaxation and the electrical conductivity. Again, an "Arrhenius" activation volume can be calculated via:

$$\Delta v_{Arr} = -kT(\partial \ln\sigma/\partial P)_T \qquad (21)$$

An updated version of the resultant activation volumes ~~are~~ is plotted in Fig. 9 where the "Arrhenius" activation volumes are plotted vs. temperature above the "central" glass transition temperature. It is apparent that for these materials the effect of pressure on the electrical relaxation time for the α relaxation is the same as that for the electrical conductivity. This represents further evidence for the importance of large scale segmental motions as regards ionic conductivity.

The strong decrease of the "Arrhenius" activation volume with increasing temperature is a consequence of the VTF-type behavior of the conductivity. Specifically, it follows that for Arrhenius processes the activation volume scales with the Gibbs energy. That has been shown both experimentally[41] and theoretically.[42,43] Since the Gibbs energy for an Arrhenius process is calculated from the slope of a plot of $\log_{10}\sigma$ vs.

1000/T, the effective Gibbs energy for VTF behavior must decrease strongly as temperature increases, as is apparent from fig. 8. Thus, the "Arrhenius" activation volume is expected to decrease as temperature increases because it varies as the effective Gibbs energy.

It is noted that the effect of ions on the α relaxation cannot be directly observed because the glass transition is shifted to higher temperatures and thus the α relaxation, if it exists, will be masked by the high "background" conductivity. However, the effect of ions on the γ relaxation region has been directly observed. The most striking example is for PEO containing KSCN as shown in Fig. 10.[17,38] The resultant DR spectrum is much more compex than for PEO (Fig. 1b). On the other hand, PEO containing NaSCN which showed very little change in the DR region. This difference was attributed to the much large size of the potassium ion, the effect being to produce more distortion in the polymer chain. Next, when the anion was changed from SCN to ClO_4, as in PEO containing $NaClO_4$, there was a strong shift in the γ relaxation region[18]. This was clear evidence of the interaction of the anion with the polymer chain. Finally, alkaline earth salts produce large changes in the DR spectrum as shown in Fig. 11.[37] It is interesting that for the better ionic conductor, the barium salt, that the γ relaxation region is shifted to higher temperature (higher activation energy).

Recent TSDC studies[39] have indicated that the γ relaxation region actually consists of several closely spaced relaxations and it is the relative populations of these which change giving rise to the shifts in the DR spectrum. Typical results are shown in Fig. 12 where the TSDC data for PEO containing NaSCN and $NaClO_4$ are plotted. While the DR spectrum

apparently consists of one, albeit very broad, peak in the γ relaxation region,[17,18] the TSDC spectrum for the same region indicates the presence of at least three closely spaced peaks.

Finally, when ions are added to PEO, it has been shown that the real part of the dielectric constant of the solid material increases by several percent.[17] In fact, the increase is approximately that which would be expected for a mixture of salt (with dielectric constants from 5 to 10) and polymer. However, this result is for the solid which is itself a mixture of amorphous and crystalline regions and it is not clear what the dielectric constant is in the individual regions.

5. ACKNOWLEDGMENTS

This work was supported in part by the U.S. Office of Naval Research. The authors would like to thank Dr. S. G. Greenbaum of the Hunter College of CUNY, New York, NY and Dr. C. G. Andeen of Case Western Reserve University, Cleveland, OH for many helpful discussions.

6. REFERENCES

1. P. W. Atkins, Physical Chemistry, Oxford, New York, NY, 1982, p. 319.

2. D. K. Cheng, Field and Wave Electromagnetics, Addison Wesley, Reading, MA, 1983.

3. F. Kroger, The Chemistry of Imperfect Crystals, North-Holland, Amsterdam, 1964.

4. R. Solomon, A. Sher, and M. W. Muller, J. Appl. Phys., 37, 3427 (1966).

5. N. G. McCrum, B. E. Read, and G. Williams, Anelastic and Dielectric Effects in Polymeric Solids, (John Wiley & Sons, New York, 1967).

6. P. Hedvig, Dielectric Spectroscopy of Polymers, (Adam Hilger Ltd., Bristol, 1977).

7. G. M. Bartenev and Yu. V. Zelenev, Editors, Relaxation Phenomena in Polymers, (John Wiley & Sons, New York, 1974).

8. N. Koizumi and T. Hanai, J. Phys. Chem. 60, 1496 (1956).

9. T. M. Connor, B. E. Read and G. Williams, J. Appl. Chem. 14, 74 (1964).

10. Y. Ishida, M. Matsuo, and M. Takayanagi, J. Polym. Sci. B3, 321 (1965).

11. K. Hikichi and J. Furuichi, J. Polym. Sci. A3, 3003 (1965).

12. K. Arisawa, K. Tsuge and Y. Wada, Jap. J. of Appl. Phys. 4, 138 (1965).

13. C. H. Porter and R. H. Boyd, Macromolecules 4, 589 (1971).

14. T. Suzuki and T. Kotaka, Macromolecules 13, 1495 (1980).

15. K. Se, K. Adachi, and T. Kotaka, Polymer Journal 11, 1009 (1981).

16. T. F. Schatzki, J. Polymer Sci., 57, 496 (1962).

17. J. J. Fontanella, M. C. Wintersgill, J. P. Calame, and C. G. Andeen,

Solid State Ionics, 8, 333 (1983).

18. M. C. Wintersgill, J. J. Fontanella, J. P. Calame, D. R. Figueroa, and C. G. Andeen, Solid State Ionics, 11, 151 (1983).

19. J. J. Fontanella, M. C. Wintersgill, J. P. Calame, D. R. Figueroa, and C. G. Andeen, In Proceedings of the 16th North American Thermal Analysis Society Conference, ed. P. J. Kelleghan, Washington, D.C., 1987, pp. 46.

20. S. G. Greenbaum, K. J. Adamic, Y. S. Pak, M. C. Wintersgill, J. J. Fontanella, D. A. Beam, and C. G. Andeen, In Proceedings of the Electrochemical Society Symposium on Electro-Ceramics and Solid State Ionics, ed. H. Tuller, Pennington, NJ, 1987, pp.

21. K. Varadarajan and R. F. Boyer, Polymer, 23, 314 (1982).

22. D. Teeters and R. Frech, Solid State Ionics, 18&19, 271 (1986).

23. S. G. Greenbaum, Y. S. Pak, M. C. Wintersgill, J. J. Fontanella, J. W. Schultz, and C. G. Andeen, J. Electrochem. Soc., 135, 235 (1988).

24. M. C. Wintersgill, J. J. Fontanella, S. G. Greenbaum, and K. J. Adamić, Br. Poly. J., to be published.

25. J. J. Fontanella, M. C. Wintersgill, M. K. Smith, J. Semancik, and C. G. Andeen, J. Appl. Phys., 60, 2665 (1986).

26. S. Havriliak and S. Negami, J. Polym. Sci. C, 14, 99 (1966).

27. M. C. Wintersgill, J. J. Fontanella, P. J. Welcher, and C. G. Andeen, J. App. Phys., 58, 2875 (1985).

28. J. J. Fontanella, M. C. Wintersgill, J. P. Calame, M. K. Smith, and C. G. Andeen, Solid State Ionics, 18&19, 253 (1986).

29. B. L. Papke, M. A. Ratner, and D. F. Shriver, J. Electrochem. Soc. 129, 1694 (1982).

30. J. J. Fontanella, M. C. Wintersgill, J. P. Calame, F. P. Pursel, D. R.

Figueroa, and C. G. Andeen, Solid State Ionics, 9&10, 1139 (1983).

31. M. C. Wintersgill, J. J. Fontanella, P. J. Welcher, J. P. Calame, and C. G. Andeen, IEEE Trans EI, 20, 943 (1985).

32. R. F. Boyer, Rubber Rev., 35, 1303 (1963).

33. B. Valeur, J. Jarry, F. Geny, and L. Monnerie, J. Polymer Sci.: Polymer Phys., 13, 667 (1975).

34. B. Valeur, L. Monnerie, and J. Jarry, J. Polymer Sci.: Polymer Phys., 13, 675 (1974).

35. E. A. Rietman, M. L. Kaplan, and R. J. Cava, Solid State Ionics, 17, 67 (1985).

36. E. Bortel, R. Lamot, M. Pulit, and Z. Sulek, Polish J. Chem., 56, 1537 (1982).

37. J. J. Fontanella, M. C. Wintersgill, J. P. Calame, and C. G. Andeen, J. Poly. Sci. Polym. Phys., 20, 113 (1985).

38. J. P. Calame, J. J. Fontanella, M. C. Wintersgill, and C. G. Andeen, J. Appl. Phys., 58, 2811 (1985).

39. D. R. Figueroa, J. J. Fontanella, M. C. Wintersgill, J. P. Calame, and C. G. Andeen, Solid State Ionics, to be published.

40. S. M. Ansari, M. Brodwin, M. Stainer, S. D. Druger, M. A. Ratner, and D. F. Shriver, Solid State Ionics, 17, 101 (1985).

41. J. J. Fontanella, M. C. Wintersgill, A. V. Chadwick, R. Saghafian, and C. G. Andeen, J. Phys. C: Solid St. Phys., 14, 2451 (1981).

42. C. P. Flynn, Point Defects and Diffusion, Oxford, Clarendon, 1972.

43. P. A. Varotsos and K. D. Alexopoulos, Thermodynamics of Point Defects and Their Relation with Bulk Properties, North-Holland, Amsterdam, 1986.

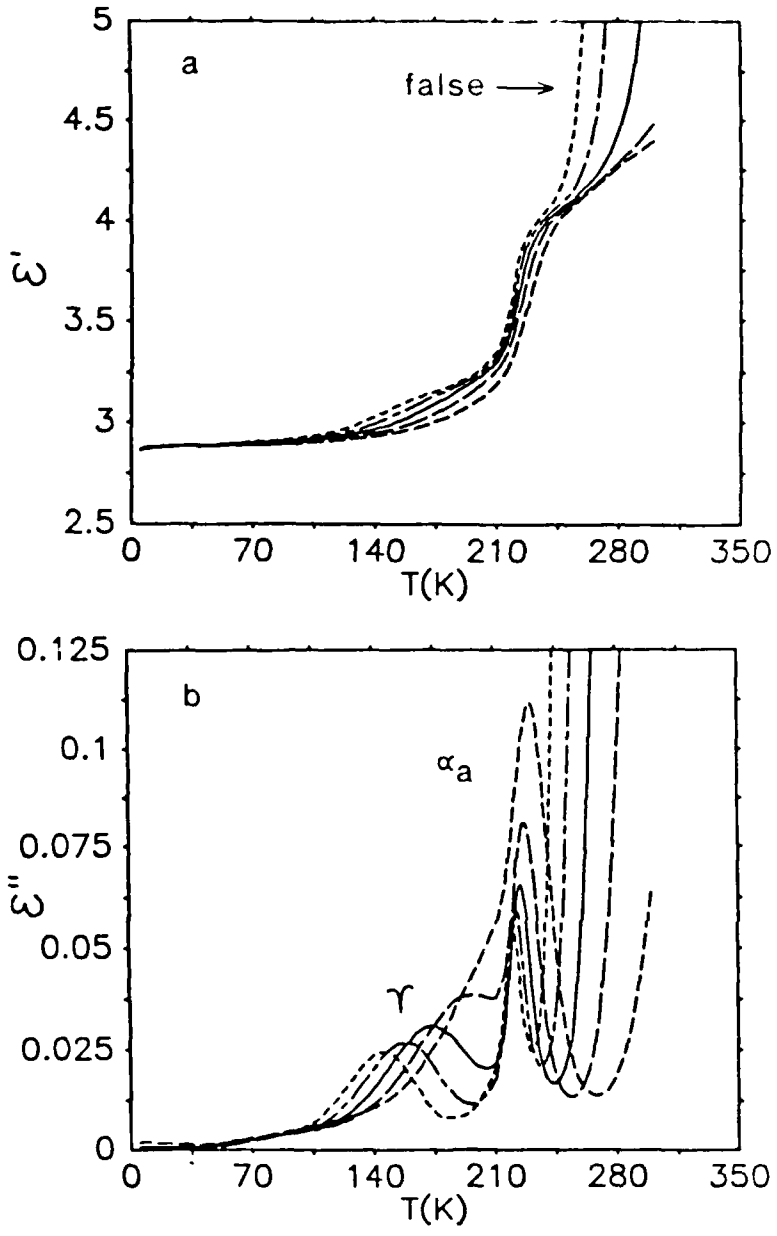

Figure 1. (a) Real and (b) imaginary parts of the dielectric constant vs. T(K) for PEO with molecular weight 4×10^6. The curves (from left to right) are: short dash-10 Hz; chain link-10^2 Hz; solid-10^3 Hz; long dash-10^4 Hz; medium dash-10^5 Hz. Straight line segments connect the datum points which are not shown. The data are the same as shown in ref. 27 on a different scale and with a different frequency designation.

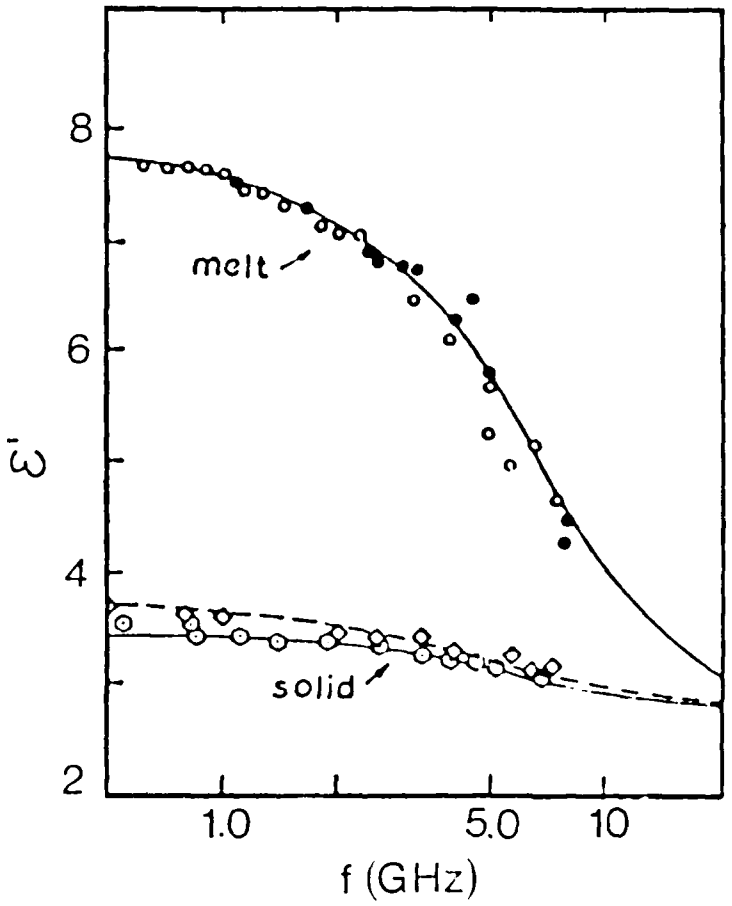

Figure 2. Real part of the dielectric constant vs. T(K) for PEO (Carbowax 20M): molten at 65.7°C (●,o); rapidly quenched crystalline (≈80%) solid (◇); slowly cooled crystalline (80%+) solid (◎). The results are from ref. 13 by permission of the author.

Figure 3. Real (a) and imaginary (b) parts of the dielectric constant at five frequencies (features from left to right): 10 Hz-short dashed lines; 100 Hz-long dased lines; 1000 Hz-solid lines; 10,000 Hz-dot dash (chain) lines; 100,000 Hz-dotted lines. Straight line segments connect the datum points. Curve (c) is a TSDC spectrum. A voltage of 200 V was applied to the sample for 15 min at a polarization temperature of 190K and the heating rate was 6 K/min.

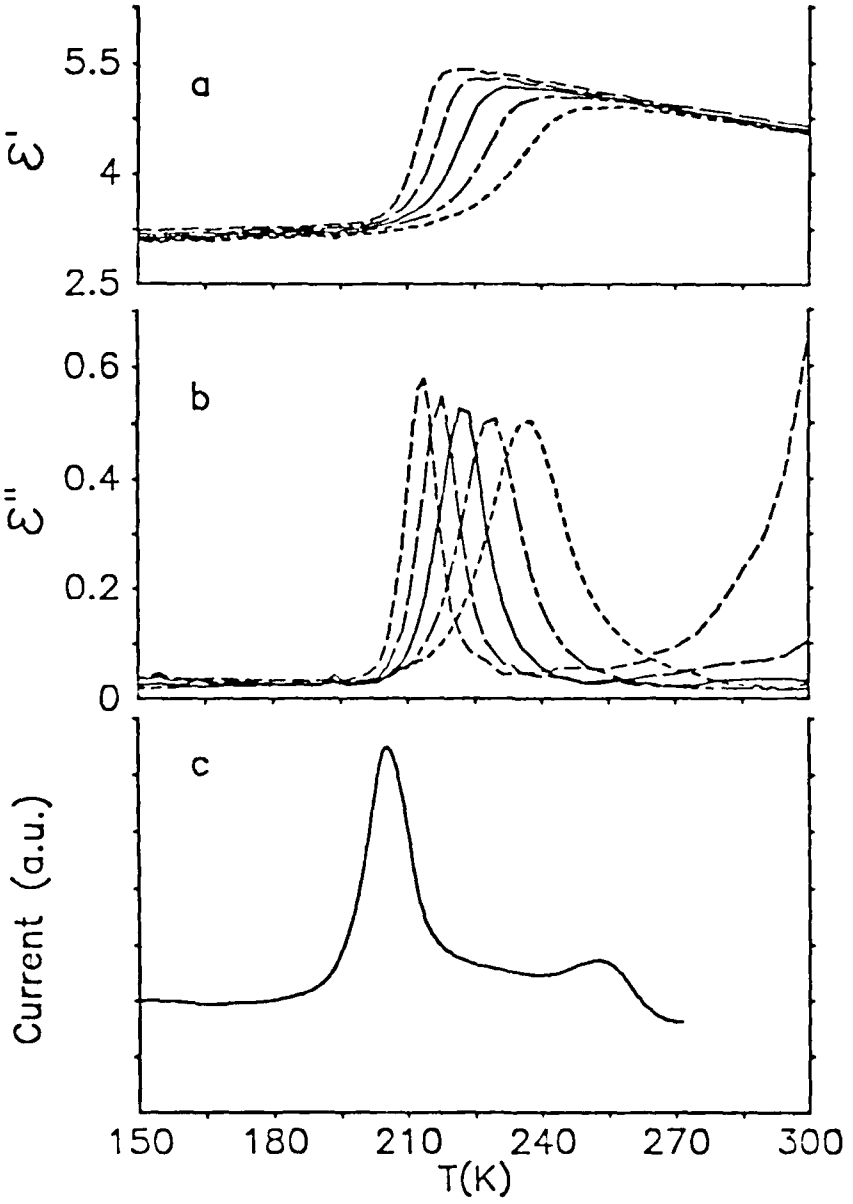

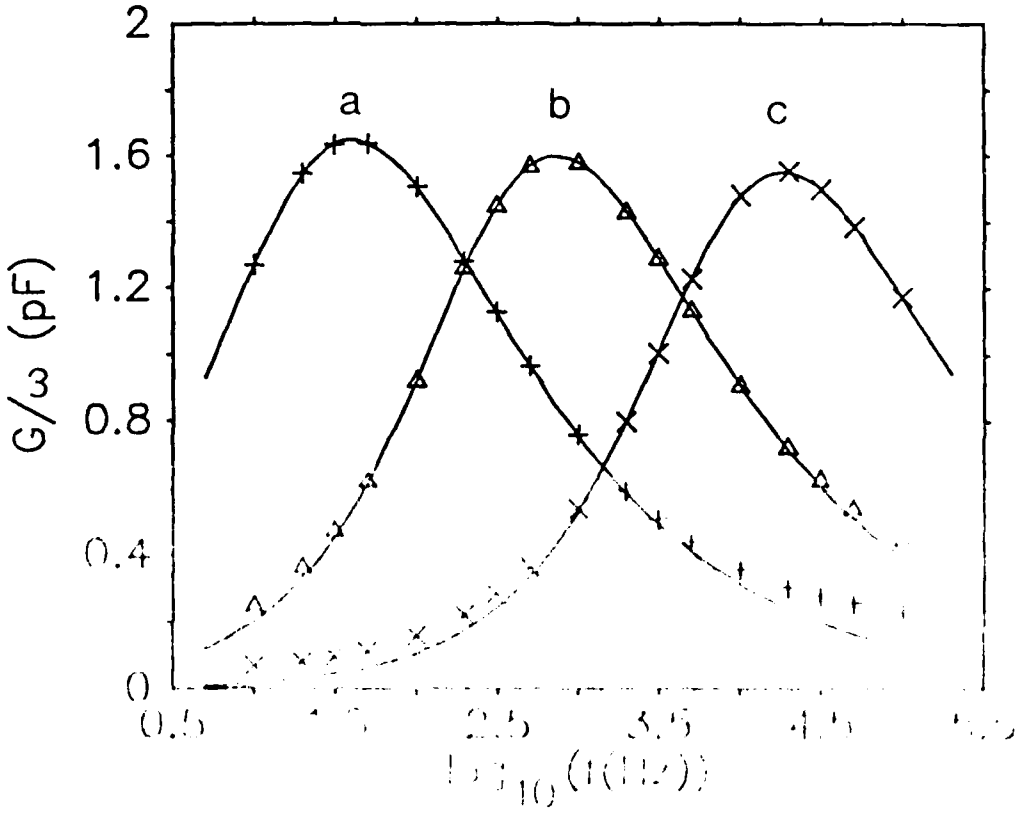
2
1.6
1.2
0.8
0.4
0
G/ω (pF)
a
b
c
0.5
2.5
3.5
log10(f(Hz))

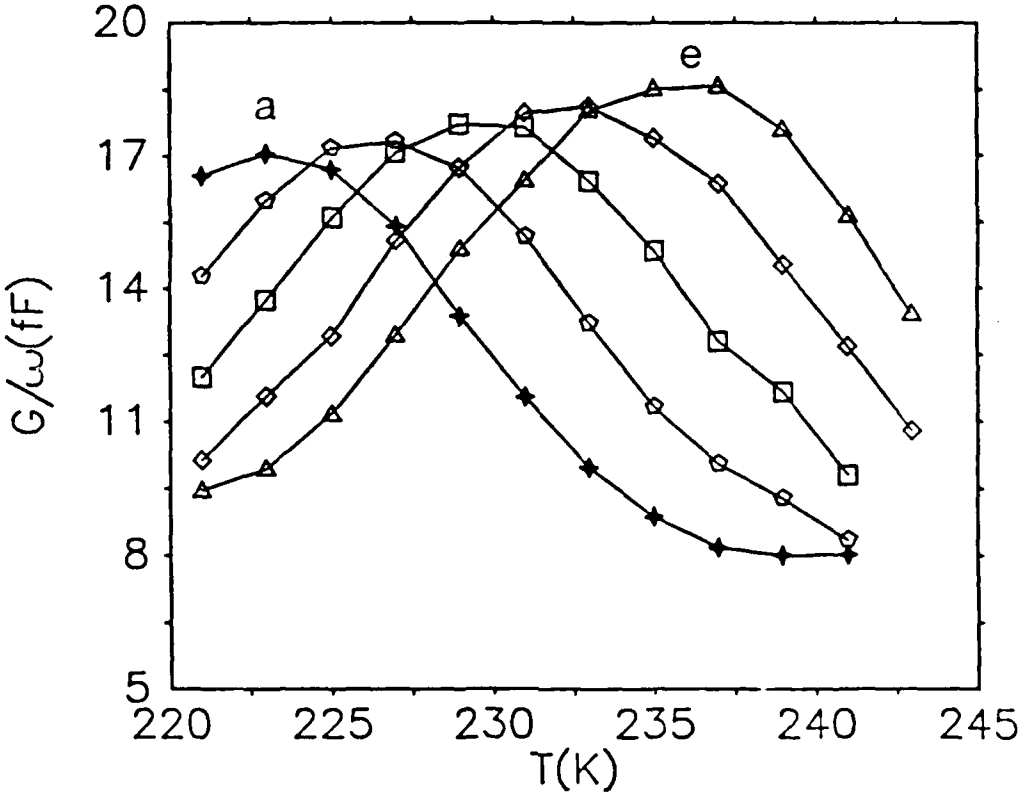

Figure 5. Dielectric loss peaks for PEO at five pressures at 1000 Hz in the region of the glass transition for molecular weight 5×10^6. The curves (from left to right) are: (a) 0.0001 (1 atm.), (b) 0.04, (c) 0.08 (d) 0.12, and (e) 0.16 GPa. Straight line segments connect the datum points. The data are from ref. 27.

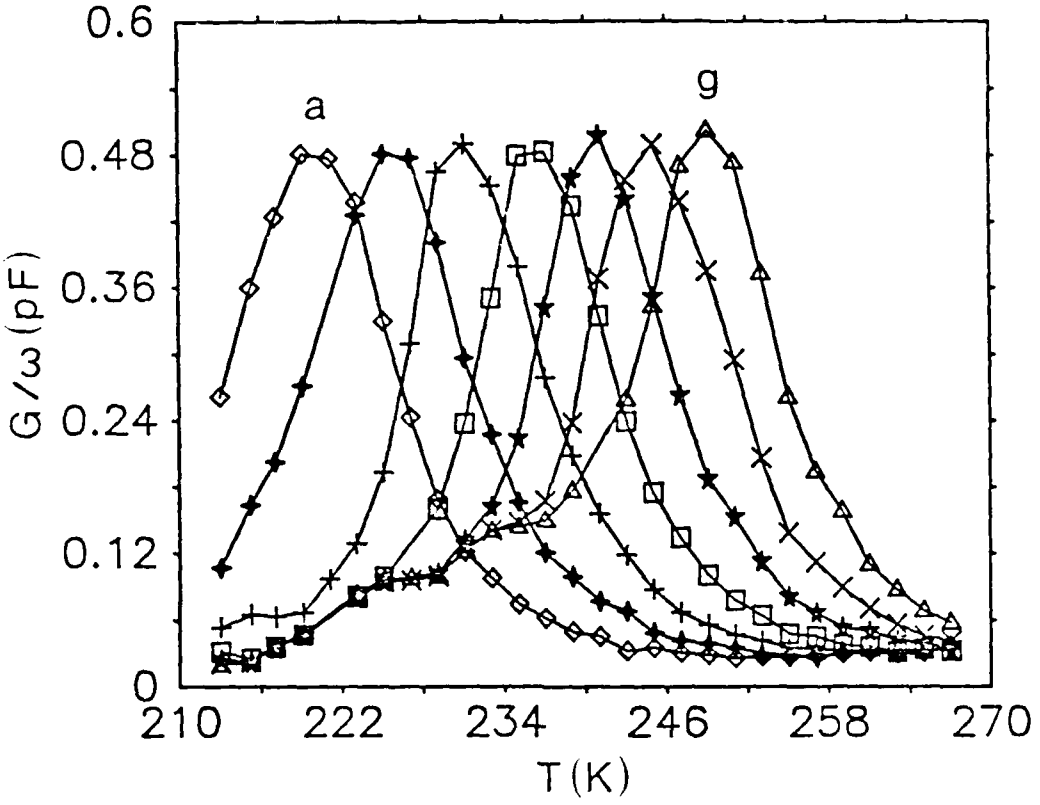

Figure 6. Dielectric loss peaks for PPO at seven pressures at 1000 Hz in the region of the glass transition. The curves (from left to right) are: (a) 0.0001 (1 atm.), (b) 0.03, (c) 0.06 (d) 0.09, (e) 0.12 GPa, (f) 0.15, and (g) 0.21 GPa. Straight line segments connect the datum points. The data are from ref. 28 which did not specify the frequency.

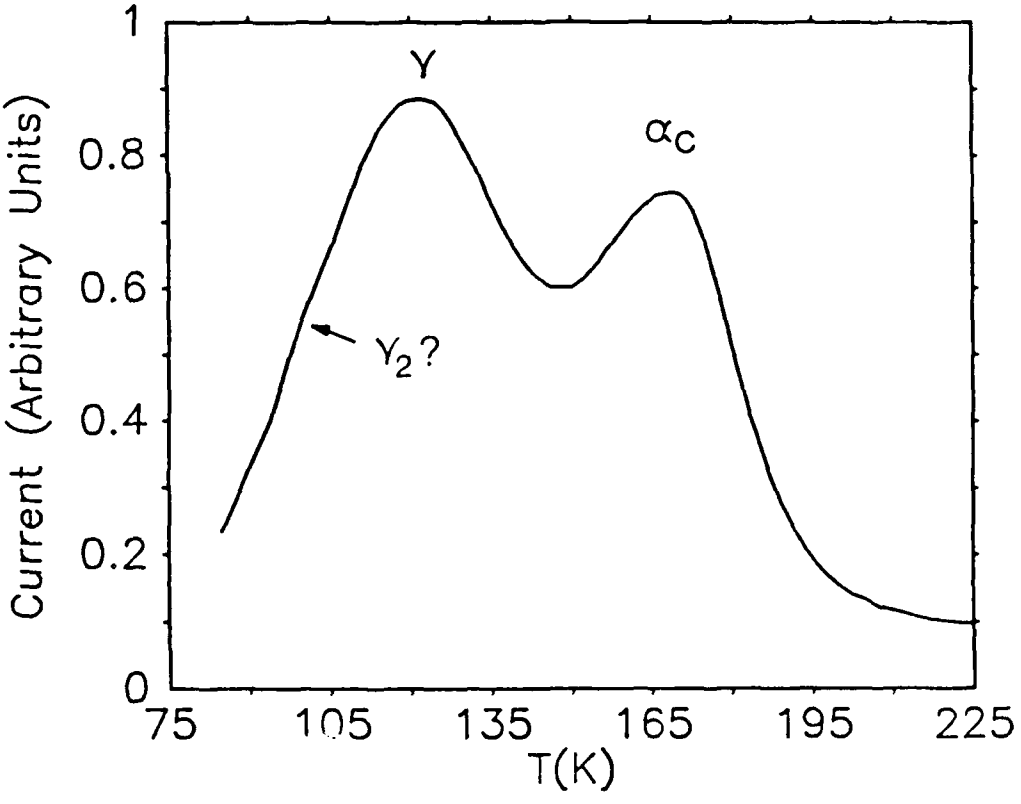

Figure 7. Low-temperature TSDC spectrum for PEO with a molecular weight of $5x10^6$. The polarization temperature was 163K and the applied voltage was 300 V for 10 min. The sweep rate was 6.13 K/min.

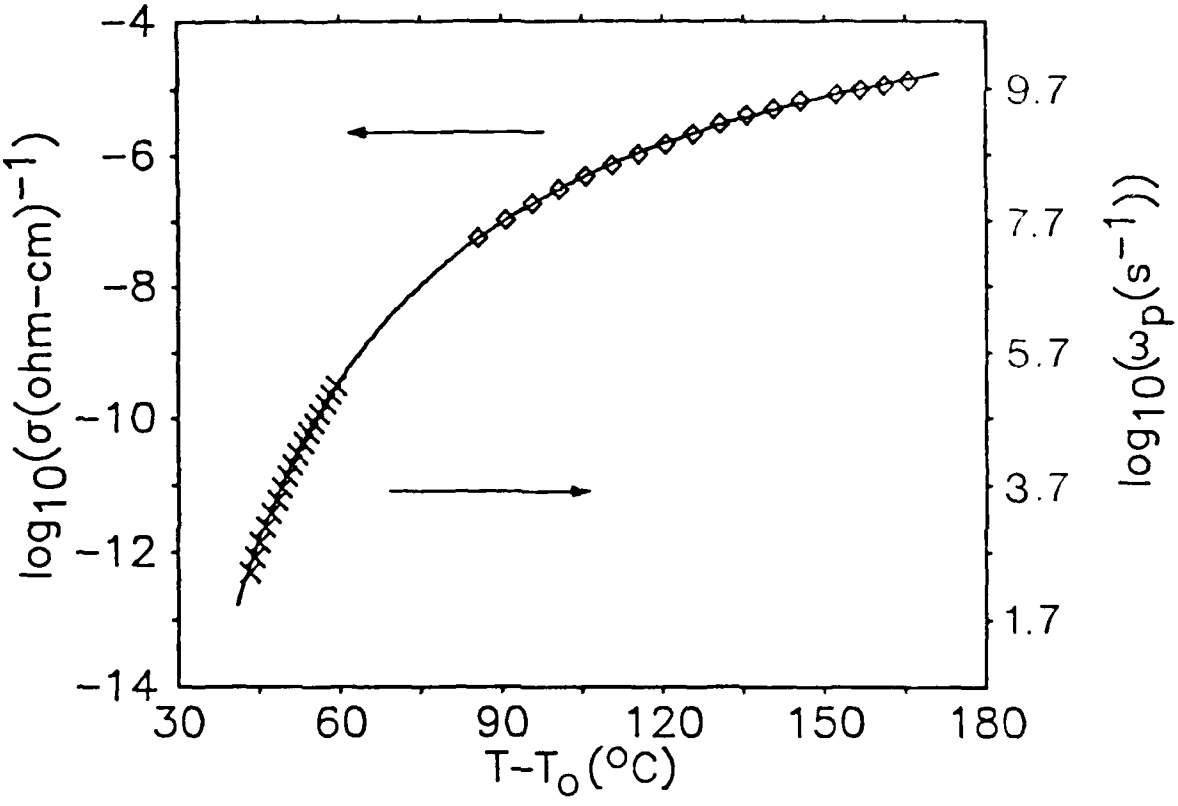

Figure 8. Electrical conductivity data for PPO-$LiCF_3SO_3$ (electrolyte composition - PPO/salt = 8:1) and peak position for the α relaxation for PPO plotted vs. temperature relative to T_o. The solid line is the VTF equation best fit to the electrical conductivity data only. The data appear in various plots in refs. 25 and 28.

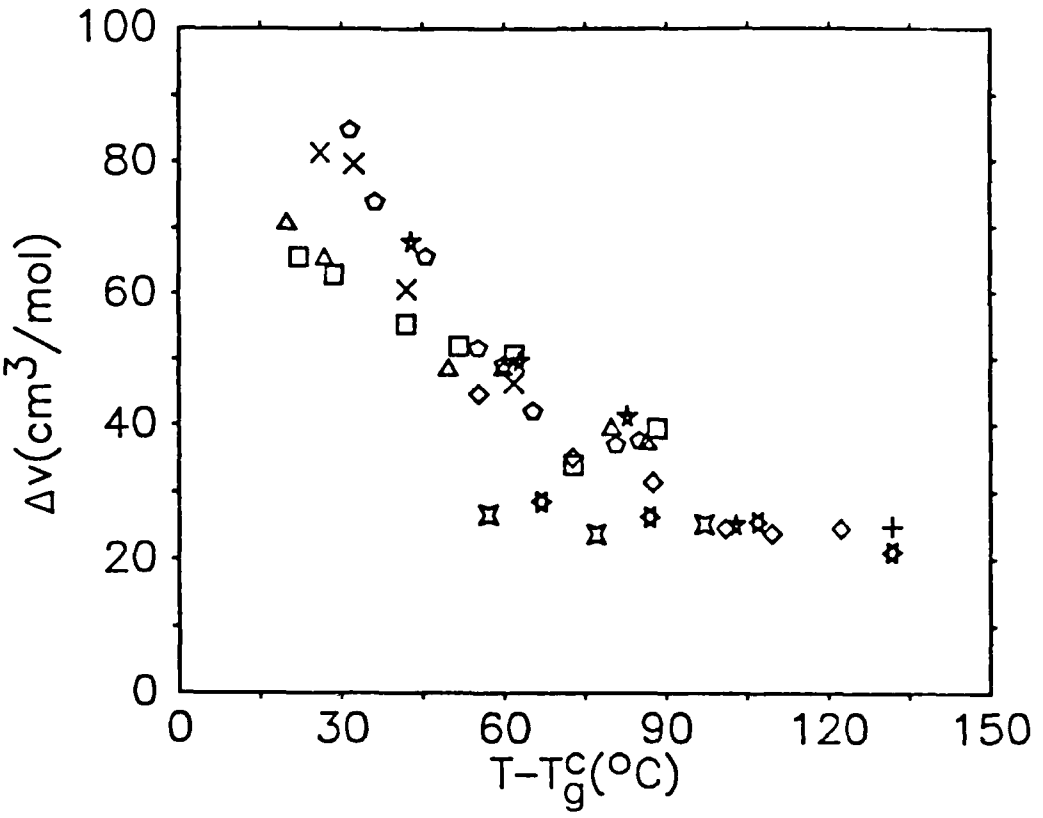

Figure 9. Activation volume vs. temperature relative to the "central" glass transition temperature; PPO-$LiCF_3SO_3$ (◇), PPO-$LiClO_4$ (□), PPO-LiI (△), uncomplexed PPO α relaxation time (x), PPO-LiSCN (⋈), PPO-$NaClO_4$ (⬠), PPO-NaI (★), PPO-NaSCN (electrical conductivity (✡), ^{14}C and ^{22}Na radio tracer measurements (+), C. Bridges and A. V. Chadwick, Solid State Ionics, to be published). Electrolyte composition ~ PPO/salt = 8:1. This figure is from ref. 20.

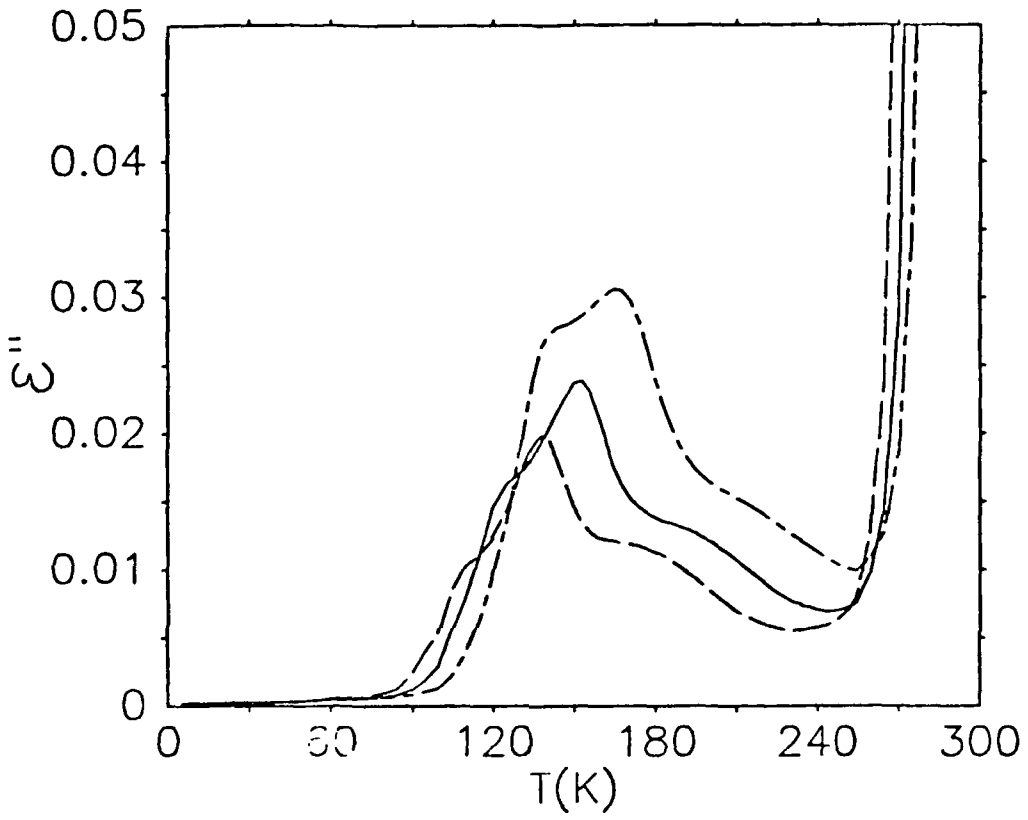

Figure 10. Imaginary part of the dielectric constant vs. T(K) for PEO-KSCN with electrolyte composition - PEO/salt = 4.5:1. The data are long dash-10^2 Hz, solid-10^3 Hz, and chain link-10^4 Hz. Straight line segments connect the datum points which are not shown. This figure is from ref. 17.

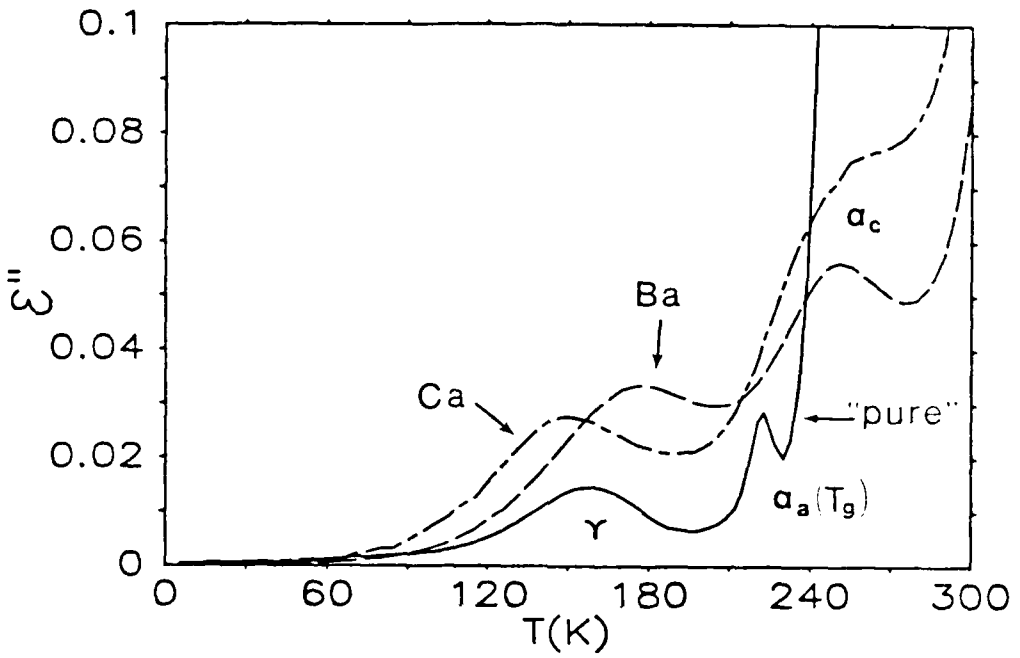

Figure 11. Imaginary part of the dielectric constant vs. T(K) at 100 Hz for various materials: Solid-PEO; Chain link-PEO-$Ca(SCN)_2$:$4H_2O$; Dash-PEO-$Ba(SCN)_2$:$3H_2O$ (electrolyte compositions - PEO/salt = 6.5:1). Straight line segments connect the datum points which are not shown. The data are from ref. 37.

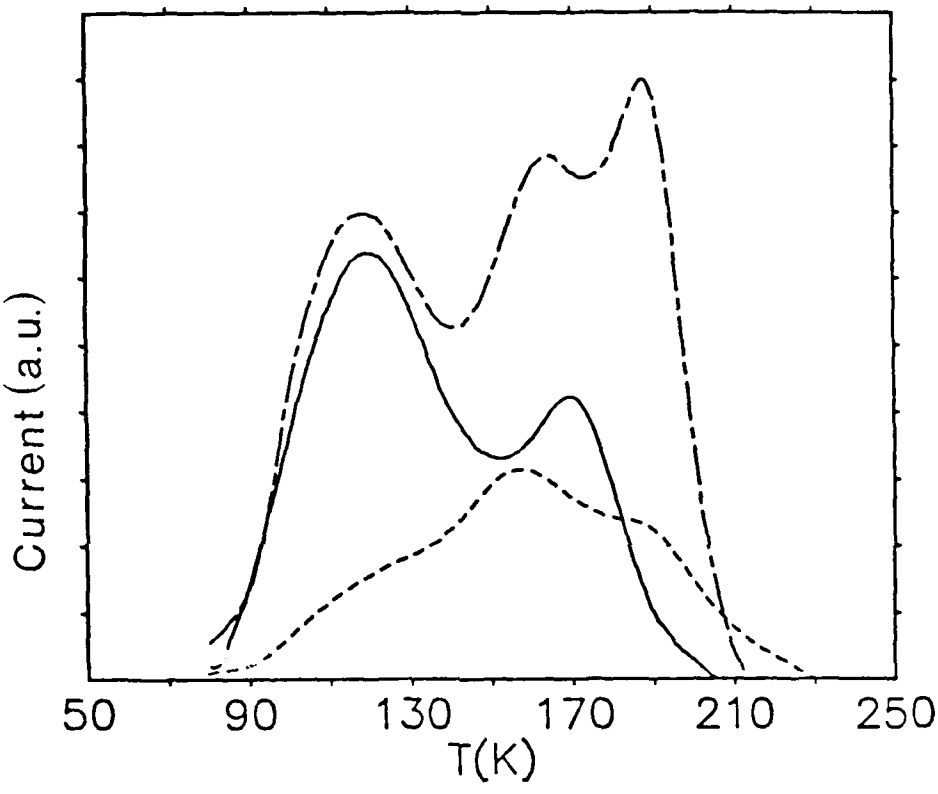

Figure 12. TSDC spectra for: (a) uncomplexed PEO--solid line, (b) PEO - NaSCN--chain link, and (c) PEO - $NaClO_4$--dash. The strength for one material relative to another is not significant. Electolyte composition - PEO/salt = 4.5:1. This figure is from ref. 39.

DL/1113/87/2

TECHNICAL REPORT DISTRIBUTION LIST, GEN

	No. Copies
Office of Naval Research Attn: Code 1113 800 N. Quincy Street Arlington, Virginia 22217-5000	2
Dr. Bernard Douda Naval Weapons Support Center Code 50C Crane, Indiana 47522-5050	1
Naval Civil Engineering Laboratory Attn: Dr. R. W. Drisko, Code L52 Port Hueneme, California 93401	1
Defense Technical Information Center Building 5, Cameron Station Alexandria, Virginia 22314	12 high quality
DTNSRDC Attn: Dr. H. Singerman Applied Chemistry Division Annapolis, Maryland 21401	1
Dr. William Tolles Superintendent Chemistry Division, Code 6100 Naval Research Laboratory Washington, D.C. 20375-5000	1
Dr. David Young Code 334 NORDA NSTL, Mississippi 39529	1
Naval Weapons Center Attn: Dr. Ron Atkins Chemistry Division China Lake, California 93555	1
Scientific Advisor Commandant of the Marine Corps Code RD-1 Washington, D.C. 20380	1
U.S. Army Research Office Attn: CRD-AA-IP P.O. Box 12211 Research Triangle Park, NC 27709	1
Mr. John Boyle Materials Branch Naval Ship Engineering Center Philadelphia, Pennsylvania 19112	1
Naval Ocean Systems Center Attn: Dr. S. Yamamoto Marine Sciences Division San Diego, California 91232	1